ADVANCED FUNCTIONAL MATERIALS

Role of Dimensionality on the Two-Photon Absorption Response of Conjugated Molecules: The Case of Octupolar Compounds**

By *David Beljonne*,* *Wim Wenseleers*, *Egbert Zojer*, *Zhigang Shuai*, *Henryk Vogel*, *Stephanie J. K. Pond*, *Joseph W. Perry*, *Seth R. Marder*, and *Jean-Luc Brédas*

A comparative study of the two-photon absorption (TPA) properties of octupolar compounds and their dipolar one-dimensional counterparts is presented on the basis of correlated quantum-chemical calculations. The roles of dimensionality and symmetry are first discussed on the basis of a simple exciton picture where the ground-state and excited-state wavefunctions of three-arm octupolar systems are built from a linear combination of the corresponding single-arm wavefunctions. This model predicts a factor of 3 increase in the TPA cross section in the limiting case of three independent charge-transfer pathways. When taking into account the full chemical structures of representative octupolar molecules, the results of the calculations indicate that a much larger enhancement associated with an increase in dimensionality and delocalization can be achieved when the core of the chromophore allows significant electronic coupling among the individual arms. These theoretical predictions are in agreement with the experimental determination of the TPA cross sections for crystal violet and the related compound, brilliant green, and suggest new strategies for the design of conjugated materials with large TPA cross sections.

1. Introduction

Two-photon absorption (TPA) is a process in which an atom or a molecule *simultaneously* absorbs two photons, which can have the same or different energies. As a result, the species reaches a (two-photon symmetry-allowed) excited state that is higher than the ground state by the sum of energies of the two absorbed photons. This process is rather inefficient and only occurs to an appreciable extent in the presence of intense laser pulses. Many applications now envisioned for two-photon absorption materials rely on processes in which TPA is followed by a second step, giving rise to a specific effect. For example, in the case where TPA is followed by internal conversion to an emissive singlet excited state, radiative decay from that excited state back to the ground state (i.e., light emission) can be exploited, namely for biomedical imaging.

[*] Dr. D. Beljonne, Dr. E. Zojer,[+] Dr. Z. Shuai,[++] Prof. J.-L. Brédas
Chemistry of Novel Materials
Center for Research in Molecular Electronics and Photonics
University of Mons-Hainaut
Place du Parc 20, B-7000 Mons (Belgium)
E-mail: david@averell.umh.ac.be

Dr. D. Beljonne, Dr. W. Wenseleers, Dr. E. Zojer, Dr. H. Vogel, Dr. S. J. K. Pond, Prof. J. W. Perry, Prof. S. R. Marder, Prof. J.-L. Brédas
Department of Chemistry, The University of Arizona
Tucson, AZ 85721-0041 (USA)

[+] Second address: Advanced Materials Division, Institute of Solid State Physics, Graz University of Technology, Petersgasse 16, A-8010 Graz, Austria.

[++] Second address Center for Molecular Science, Institute of Chemistry, The Chinese Academy of Sciences, Beijing 100080, People's Republic of China.

[**] The work in Mons is carried out within the framework of the Belgium Prime Minister Office of Science Policy program "Pôle d'Attraction Interuniversitaire en Chimie Supramoléculaire et Catalyse (PAI 4/11)" and is partly supported by the Belgium National Fund for Scientific Research (FNRS-FRFC). DB is Chercheur Qualifié FNRS. The work at Arizona is partly supported by ONR and the IBM-SUR program. EZ acknowledges support by the Spezialforschungsbereich Elektroaktive Stoffe.

Conventional one-photon linear absorption spectroscopy can be used to generate excited states that in turn can initiate specific reactions or processes. However, while the transition probability for one-photon absorption is linearly proportional to light intensity, that for the simultaneous absorption of two identical photons depends on the square of light intensity, I^2. Such a quadratic dependence provides the ability to localize the excitation with high 3D spatial resolution in the focus of a laser beam, one of the main advantages of two-photon absorption. Another major feature is that the linear absorption of a material can be very weak in the wavelength range where two-photon absorption occurs, thereby allowing excitation of the materials at greater depth than might be possible via one-photon excitation. These are clear advantages for applications such as imaging in absorbing or scattering media, for example biological tissues. Also, highly transparent nonlinear absorptive materials are of great interest in optical-limiting applications.

In the past, two-photon absorption has often been regarded as an adverse effect by the nonlinear optics community. This is especially true in the case of all-optical switching where two-photon absorption leads to optical loss and damage. Consequently, for a long time, efforts were made to minimize two-photon absorption. However, as is often the case, what can be regarded as highly detrimental in a given context, can be exploited in other fields. Molecules with a large two-photon absorption response are now in great demand for a variety of applications, including two-photon excited fluorescence microscopy,[1,2] optical limiting,[3–5] three-dimensional optical data storage,[6,7] two-photon induced biological caging studies,[8] and nano- or microfabrication.[9] Unfortunately, until recently, criteria for the design of molecules with large TPA coefficient had not been well-developed.[10]

Recently, we proposed new strategies for the molecular engineering of high TPA cross-section materials. These include the design of: i) centrosymmetric molecular architectures of the

  1616-301X/02/0909-0631 $ 17.50+.50/0

type D–π–A–π–D or A–π–D–π–A (where D denotes an electron-donor group, A an electron-acceptor group, and π is a conjugated segment) wherein the TPA enhancement upon substitution stems from the photoinduced drift in electron density from the donor to the acceptor along a quadrupolar path;[11,12] and ii) non-centrosymmetric dipolar D-π–A structures where the origin of the high TPA response in the lowest excited state lies in the one-dimensional charge transfer from the donor to the acceptor across the conjugated bridge as one drives the geometric structure partly towards the cyanine limit.[13]

Here, we extend our analysis to compounds with increased dimensionality. As a first step, we focus our attention on octupolar molecules where charge transfer upon photoexcitation can occur along three different axes, a feature that could enhance the TPA response. Since the pioneering work of Zyss and co-workers some ten years ago,[14,15] compounds with octupolar symmetry have been of interest for second-order nonlinear optical applications.

The potential interest of octupolar systems for TPA arises from the fact that second-harmonic generation (SHG) measurements indicate that strong two-photon resonances usually occur with several low-lying excited states;[15] moreover, strong in–out polarization of the π-electronic cloud (with drift of the electron density from the core to the periphery or vice versa) has been calculated for these excited states.[16] In linear quadrupolar systems, such a centrosymmetric charge redistribution has been shown to induce a significant enhancement in TPA cross section.[11,12] Recent experimental and theoretical works have confirmed that octupolar structures are attractive materials for second-order and third-order nonlinear optical applications, including TPA;[17–19] interestingly, it was shown that the TPA cross section into the lowest excited state scales with the second-order molecular polarizability as found previously for dipolar architectures.[13] In the context of developing a better understanding of structure–property relationships for TPA and of the role of dimensionality, octupolar systems offer the possibility of investigating the influence of the presence of *three* axes for charge transfer and electronic redistribution in the excited states.

The interplay and extent of coupling among these three axes of charge transfer is expected to influence significantly the nonlinear optical response. Therefore, we found it useful to apply the basic concepts of molecular exciton theory to characterize this coupling. After a brief discussion of the theoretical methodology (Sec. 2), we describe the exciton molecular theory as applied to octupolar structures in Section 3; this approach enables us to relate the magnitude of the TPA response to the strength of the coupling between the three arms of an octupolar chromophore. In Section 4, we consider a number of representative octupolar molecules, for which correlated quantum-chemical calculations are performed by taking into account the full chemical structure. Comparison between the results of these calculations and the predictions from exciton theory provides insight into the origin of the TPA response in octupolar architectures and suggests new routes to optimized TPA chromophores. To check these ideas, we present in Section 5 an experimental investigation of the nonlinear absorption in crystal violet and a related compound, brilliant green.

2. Theoretical Methodology

The two-photon absorption cross-section, δ, is given (in vacuum) by:[13,20]

$$\delta = \frac{3}{2}\frac{\hbar\omega^2\,\mathrm{Im}\left[\,\gamma(-\omega;\omega,\omega,-\omega)\,\right]}{\varepsilon_0 c^2} \tag{1}$$

where $\gamma(-\omega;\omega,\omega,-\omega)$ is the third-order molecular polarizability, $\hbar\omega$ the energy of the incoming photons, and ε_0 the vacuum electric permittivity. Equation 1 implies that the absorbed photons are of the same energy. The methodology adopted here to calculate the third-order molecular polarizability has been described in detail previously.[11–13,21,22] We recall that this formalism is based on a perturbation treatment of the interaction between light and matter, which provides expressions for the molecular polarizabilities in the form of a summation over all electronic excited states of the molecule (sum-over-states, SOS, approach).[23]

In many cases, the full SOS expression for the third-order polarizability can be simplified; this is especially true when a single low-lying excited state, $|e\rangle$, dominates the linear optical response.[24] In that case, the summations over the excited states that are (electric-dipole) coupled to the ground state $|g\rangle$ can be limited to that excited state alone and the summations over upper-lying excited states go over those few excited states $|e'\rangle$ that are strongly coupled to $|e\rangle$. The longitudinal (i.e., along the main chain axis) component of the frequency-dependent third-order molecular polarizability, $\gamma_{xxxx}(-\omega;\omega,\omega,-\omega)$, then reduces to:

$$\gamma_{xxxx}(-\omega;\omega,\omega,-\omega) \approx \frac{1}{6\hbar^3} P(-\omega;\omega,\omega,-\omega) \left[\begin{array}{ll} \dfrac{M_{ge}^2 \Delta\mu_{ge}^2}{(E_{ge}-\hbar\omega-i\Gamma_{ge})(E_{ge}-2\hbar\omega-i\Gamma_{ge})(E_{ge}-\hbar\omega-i\Gamma_{ge})} & D \\ -\dfrac{M_{ge}^4}{(E_{ge}-\hbar\omega-i\Gamma_{ge})(E_{ge}-\hbar\omega-i\Gamma_{ge})(E_{ge}+\hbar\omega-i\Gamma_{ge})} & N \\ +\displaystyle\sum_{e'} \dfrac{M_{ge}^2 M_{ee'}^2}{(E_{ge}-\hbar\omega-i\Gamma_{ge})(E_{ge'}-2\hbar\omega-i\Gamma_{ge'})(E_{ge}-\hbar\omega-i\Gamma_{ge})} & T \end{array} \right] \tag{2}$$

where M_{ge}, $\Delta\mu_{ge}$, and E_{ge} denote the longitudinal component of the transition moment, the transition energy, and the dipole moment difference between the $|g\rangle$ and $|e\rangle$ states. D is called the dipolar term since it exclusively appears in non-centrosymmetric systems; its expression is similar to that of the only term appearing in the two-state expression for β, the second-order polarizability.[24,25] Term T involves upper-lying (two-photon) excited states $|e'\rangle$ and is strongly dependent on the coupling of $|e'\rangle$ with $|e\rangle$. The third term is the negative term, N, which is related to the linear polarizability. In the present work, all damping factors Γ_{gn} are set to 0.1 eV; this choice of damping factor is consistent with the width of the TPA spectra in a number of conjugated molecules and provides TPA cross sections in good agreement with experimental data for a number of

  1616-301X/02/0909-0632 $ 17.50+.50/0 *Adv. Funct. Mater.* **2002**, *12*, No. 9, September

ADVANCED FUNCTIONAL MATERIALS

conjugated molecules[11] (note that, within simplified models for TPA, the TPA cross section to excited state n is inversely proportional to Γ_{gn}, see below).

The expression for term N only allows for the possibility of one-photon resonances; therefore, this term makes no contribution to two-photon absorption. In the D and T terms, two-photon resonances occur with respect to $|e>$ and $|e'>$, respectively. In the case of resonance to $|e>$, a two-state model ($|g>$, $|e>$) is often appropriate to describe the peak TPA cross section, while (at least) three states ($|g>$, $|e>$, $|e'>$) have to be included in the SOS procedure to describe two-photon absorption into $|e'>$. Within such simplified models, Equation 2 combined with Equation 1 leads, for resonances to $|e>$ and $|e'>$, to Equations 3 and 4, respectively:

$$\delta_x^{g\to e} \propto \frac{M_{ge}^2 \, \Delta\mu_{ge}^2}{(\frac{E_{ge}}{2})^2 \Gamma} \tag{3}$$

$$\delta_x^{g\to e'} \propto \frac{M_{ge}^2 \, M_{ee'}^2}{(E_{ge} - \frac{E_{ge'}}{2})^2 \Gamma} \tag{4}$$

Here, we have assumed the same damping, Γ, for all excited states and index x refers to the longitudinal component of the TPA cross section. Note that Equation 4 is not applicable when a double resonance situation is approached, i.e., when $(E_{ge}-E_{ge'}/2) \approx \Gamma$.[13,21]

To compare the calculated δ with the value measured experimentally in solution, one needs to evaluate the orientationally averaged (isotropic) value of γ, which is defined as:

$$<\gamma> = \frac{1}{15}\sum_{ij}(\gamma_{iijj} + \gamma_{ijji} + \gamma_{ijij}) \tag{5}$$

where $i,j = x,y,z$. For (quasi-) one-dimensional molecules, Equation 5 reduces to $<\gamma> = (1/5)\gamma_{xxxx}$ while in octupolar structures the average value of the third-order molecular polarizability amounts to $(8/15)\gamma_{xxxx}$ for the xyz reference system shown in Figure 1 (this can easily be obtained from Eq. 5 when taking account of the following relations among the γ tensor components in a C_{3h} molecule: $\gamma_{xxxx} = \gamma_{yyyy}$; $\gamma_{xxyy} = (1/3)\gamma_{xxxx} = \gamma_{yyxx}$); a ratio of 8/3 is thus expected as a result of dimensionality between the isotropic γ and δ values in octupolar compounds and in the corresponding dipolar structures (note that a corresponding increase in dimensionality doubles the norm of the second-order polarizability).[16]

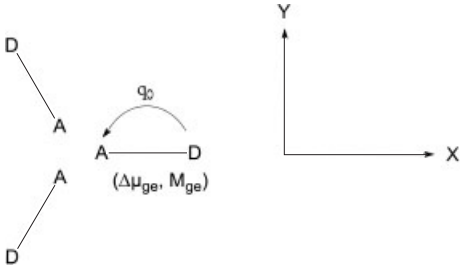

Fig. 1. Schematic representation of a C_3-symmetry molecule with three charge-transfer (CT) axes; M_{ge} and $\Delta\mu_{ge}$ denote the single arm transition dipole moment to the lowest CT excited state and the corresponding state dipole moment difference with respect to the ground state, respectively (q_0 is the amount of charge transfer in the isolated arm).

The excited-state characteristics to be plugged into the SOS expressions for the calculation of the molecular polarizabilities and the TPA cross sections have been computed by combining the intermediate neglect of differential overlap (INDO)[26] method to a multireference double configuration interaction (MRD-CI) formalism. The Mataga–Nishimoto[27] potential was adopted to describe electron–electron interactions; this parameterization was found to provide, for a series of model octupolar molecules, excitation energies and static second-order polarizabilities in better agreement with experiment than those obtained by using the Ohno–Klopman potential.[28] The MRD-CI calculations were performed on the basis of an active space, including typically from 8 to 12 π orbitals and a number of reference configurations spanning from 4 to 8, depending on molecular size and symmetry. The molecular geometries used as input in the electronic structure calculations were optimized at the Austin Model 1 (AM1)[29] level.

3. An Exciton Model for TPA in Octupoles

Octupolar molecules with C_3 or C_{3h} symmetry can be regarded as an assembly of three dipolar-like arms, see Figure 1. With each individual arm (a, b, or c) of the octupole, one can associate a dominant low-lying charge-transfer excited state, hereafter denoted a*, b*, or c*, characterized by a transition dipole moment M_{ge} and a difference in dipole moment $\Delta\mu_{ge}$ with respect to the ground state (corresponding to a charge transfer, q_0, from a donor end-group to an acceptor end-group). In the octupolar system, the excited-state wavefunctions of the individual arms form a reducible representation of the $C_{3(h)}$ symmetry group described by the basis (a^*, b^*, c^*). By using group theory and the Gram–Schmidt orthogonalization procedure, a new set of orthonormal symmetry-adapted wavefunctions can be constructed from the following linear combinations:

$$\frac{1}{\sqrt{3}}(a^*+b^*+c^*);\ \frac{1}{\sqrt{6}}(2\times a^*-c^*-b^*);\ \text{and}\ \frac{1}{\sqrt{2}}(b^*-c^*) \tag{6}$$

In the C_{3h} [C_3] point group, the first function belongs to the A′ [A] representation, while the other two correspond to the two components (denoted as α and β in the following) of the doubly degenerate E′ [E] representation. We stress that *both* A′ and E′ excited states are two-photon allowed, while one-photon excitations from the ground state are allowed to the E′ excited states but forbidden to the A′ state.

In the Appendix, we show how the wavefunctions of the ground state and excited states of the octupolar molecules can be built as an ad hoc linear combination of the isolated-arm wavefunctions[30] and evaluate the excited-state energies.

If the interaction between the individual arms is negligible, the excitation energies are, as expected, exactly the same as those obtained for the individual arms and the transitions from the ground state 1A′ to the 2A′ and 1E′ excited states are (acci-

  1616-301X/02/0909-0633 $ 17.50+.50/0

dentally) degenerate. In this case, *an increase by a factor of 3* of the TPA cross section of the octupole molecule with respect to the isolated arm occurs (note that a similar analysis leads to an enhancement factor 3/2 for the orientationally averaged second-order polarizability, as predicted earlier).[31]

If the arms do interact, the degeneracy of the lowest A′ and E′ excited states is lifted; when denoting V the coupling energy between excited states localized on separate arms, the 2A′ state becomes destabilized by an energy $2V$ and the 1E′ state becomes stabilized by an energy $-V$ (see Eq. A6 in the Appendix).

The expressions for the TPA cross sections into the 1E′ and 2A′ excited states can then be written as (see Appendix):

$$\delta_{1E'} \propto \frac{3}{8}\frac{M_{ge}^2 \Delta\mu_{ge}^2}{(\frac{E_{ge}-V}{2})^2 \Gamma}; \qquad \delta_{2A'} \propto \frac{6}{8}\frac{M_{ge}^2 \Delta\mu_{ge}^2}{(\frac{E_{ge}}{2}-2V)^2 \Gamma} \tag{7}$$

where M_{ge}, $\Delta\mu_{ge}$, and E_{ge} refer to the transition parameters for an isolated arm. It is interesting to note that from Equation 7 we expect (for positive V values) a larger TPA intensity into the 2A′ state than in the 1E′ state, as a result of a more favorable detuning factor; the ratio between δ in 2A′ and 1E′ is $2(E_{ge}-V)^2/(E_{ge}-4V)^2$. We note that if V were to approach $E_{ge}/4$, the energies of the lowest two excited states become $E(1E') \sim E_{ge} - E_{ge}/4$ and $E(2A') \sim E_{ge} + 2 \times E_{ge}/4$ and therefore $E(2A') \sim 2 \times E(1E')$, i.e., it corresponds to a double resonance situation.

Two other features about Equation 7 are worth stressing:

- For resonance to the 2A′ state, although the two-photon absorption process involves an intermediate state, 1E′, that is different from the target state (as is the case in the centrosymmetric quadrupolar molecules),[11] *the magnitude of δ within this exciton picture relates primarily to the amount of photoinduced charge transfer, $\Delta\mu_{ge}$, along the individual arms*, a situation which is typical of dipolar architectures.[13,19] The recipes that have been followed to maximize the second-order response in one-dimensional push–pull compounds are therefore also expected to apply to δ.
- One can take advantage of the inter-arm coupling to optimize the detuning factor and boost the TPA response associated with the 2A′ excited state. For instance, if $E_{ge} = 2.5$ eV and $V = 0.3$ eV (realistic values for some conjugated octupoles, see below), the TPA cross section in the 2A′ state is predicted (Eq. A9 in the Appendix) to increase by about a factor of 5 with respect to that in the corresponding dipolar chromophore.

This analysis confirms that octupolar compounds are potentially interesting candidates for TPA. However, we can expect that the TPA response in octupolar compounds will be highly sensitive to the actual interactions among the individual molecular branches. Such interactions might enhance or reduce the charge transfer from the core of the three-fold symmetry structure to its periphery (or vice versa), which obviously should affect the resulting two-photon absorption cross sections; this is particularly true if there is significant delocalization across the whole molecule through the core as, for instance, in crystal violet (see below).

The nature and strength of the coupling depend on the chemical structure of the octupole and can only be gauged quantitatively by means of a "supermolecular" approach (where the wavefunctions of the electronic states are obtained by diagonalization of the entire Hamiltonian, allowing for reorganization of the electron density in the octupole with respect to the corresponding one-dimensional segments). The results of such calculations are discussed in the next section.

4. Two-Photon Absorption Cross Sections of Model Compounds

INDO/MRD-CI/SOS calculations of the TPA cross sections have been performed on: i) four model *octupolar* systems; and ii) their individual arms, which have a *dipolar* character, see Scheme 1. To allow a direct comparison between the two sets

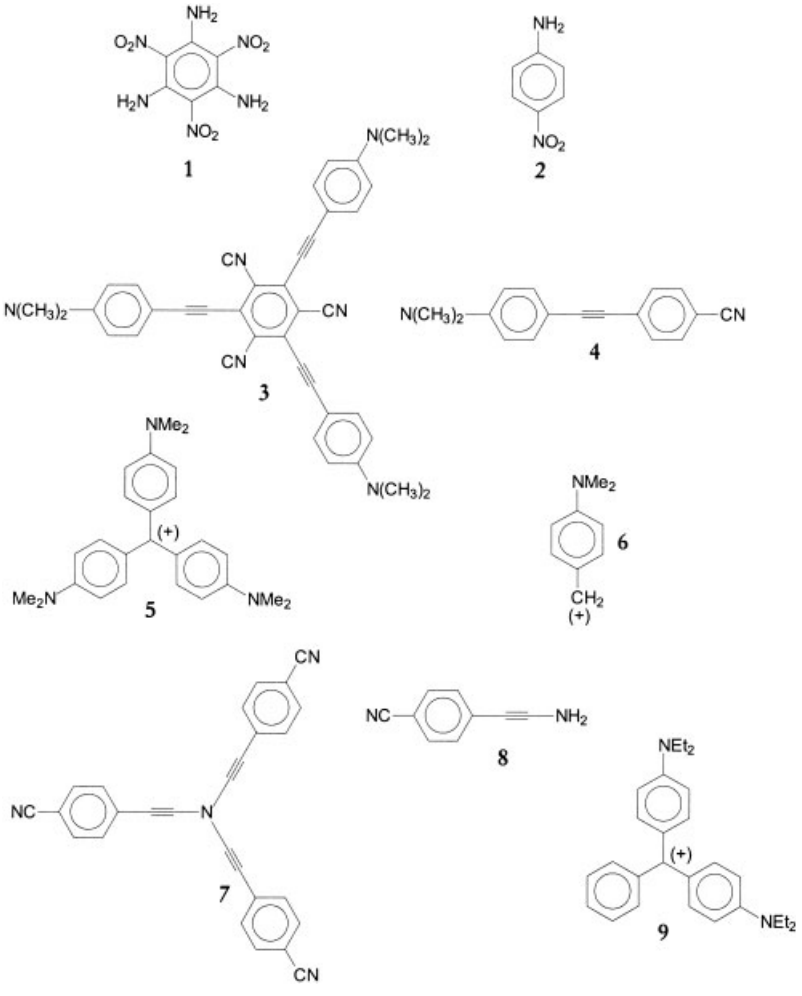

Scheme 1.

  1616-301X/02/0909-0634 $ 17.50+.50/0 *Adv. Funct. Mater.* **2002**, *12*, No. 9, September

ADVANCED FUNCTIONAL MATERIALS

of calculations, the ground-state geometry of the individual arms in the octupolar molecules was retained for the computation of the electronic excited states and two-photon absorption cross sections of the corresponding dipolar chromophores. Note that a fully planar structure was considered for **1** and **3**, which both belong to the D_{3h} point group. Crystal violet, **5**, is propeller-shaped with twist angles around the bond connecting the central carbon atom to the phenylene rings on the order of 30°; the symmetry is reduced to D_3, but the in-plane components of the γ-tensor largely dominate the nonlinear response, so that the analysis described in Section 3 still applies.

The (longitudinal) dipole matrix elements and excitation energies, as calculated for the octupolar chromophores at the INDO/MRD-CI level and on the basis of the exciton theory developed above, are listed in Table 1; the molecular parameters provided by the INDO/MRD-CI calculations on the corresponding dipolar arms are also reported. Note that we found an overall good agreement between the measured and calculated excitation energies and second-order molecular polarizabilities in all octupoles.[32] In Figures 2–5, the TPA spectra simulated for the octupolar molecules and the corresponding dipolar arms are compared; the δ values computed for the octupolar structures are listed in Table 2. From these results, distinct behaviors can be distinguished:

i) In triaminotrinitrobenzene, **1**, large differences are found between the values predicted from the exciton model built on the basis of the individual arms (**2** or para-nitroaniline) and those computed at the MRD-CI level. The coupling among the branches of the octupole is weak: the splitting between the E′ and A′ states is calculated to be ~–0.05 eV (this is not too surprising for side groups that are connected in meta positions of a benzene ring); as a result, from exciton theory, one would expect a TPA response three times as big in **1** as in **2**. However, the INDO/MRD-CI calculations yield similar peak δ values for the two compounds. We explain this discrepancy by the fact that modeling the electronic structure and optical properties of **1** in terms of the excited states of **2** is a very crude approximation (the chemical structure of triaminotrinitrobenzene is quite different from that of three para-nitroaniline molecules arranged in a C_3-like conformation as sketched in Fig. 1). Therefore, this couple of chromophores is unfortunately not a good choice to test the validity of the exciton model.

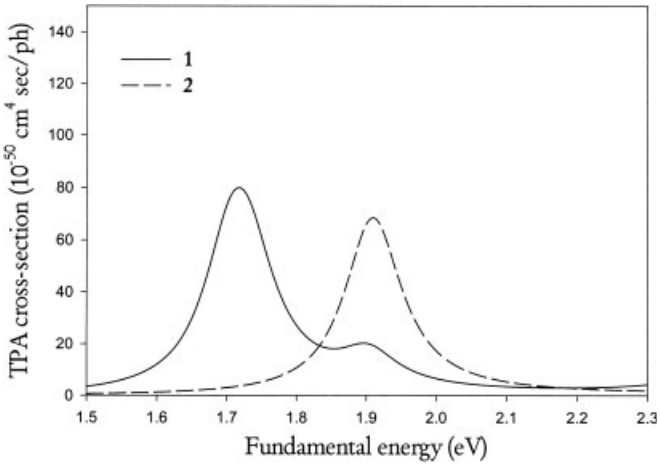

Fig. 2. INDO/MRD-CI/SOS two-photon absorption spectra of molecules **1** and **2**.

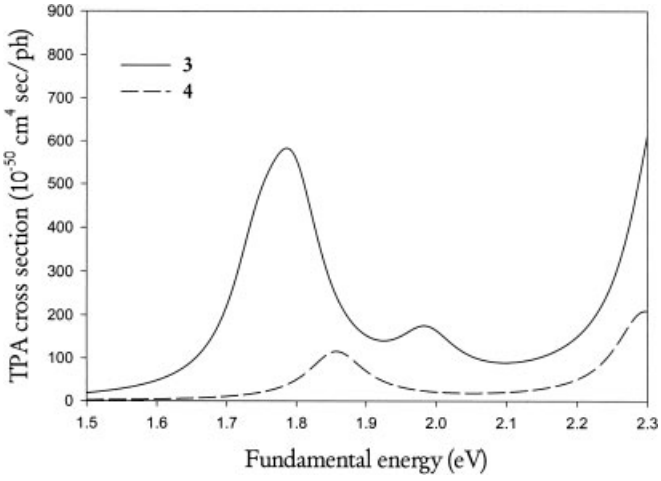

Fig. 3. INDO/MRD-CI/SOS two-photon absorption spectra of molecules **3** and **4**.

ii) As is the case for **1**, the coupling between the branches of the octupole is rather weak in **3**: the splitting between the E′ and A′ states is calculated to be ~0.1 eV. In contrast to the previous couple of compounds, the matrix elements computed for octupole **3** are slightly larger than those predicted from the exciton approach. A zero differential overlap (ZDO) analysis of the population in the 1E′ and 2A′ excited states of **3** reveals a total amount of charge transfer from each dimethylamino donor group to the cyano acceptor moiety located in the para position that is comparable to that in compound **4**, i.e., $q \approx q_0$; hence, according to the exciton model (see Appendix), the TPA response of the three-fold symmetry molecule **3** should be three times as large as that of the one-dimensional structure **4**. This is in agreement with the description provided by the supermolecular approach.

iii) In the case of chromophore **5**, crystal violet, the model assuming weak interactions among the

Table 1. INDO/MRD-CI molecular parameters calculated for compounds **1**–**8**. Capital letters refer to the dipolar arms, small letters to the octupoles. The numbers between parentheses are obtained on the basis of the exciton theory described in the text. Unless otherwise mentioned, the values for the dipole matrix elements correspond to the *x*-axis components.

Compound	E_{ge} [eV]	M_{ge} [D]	$\Delta\mu_{ge}$ [D]	ε_{ge} [eV]	$\varepsilon_{ge'}$ [eV]	m_{ge} [D]	$\delta\mu_{ge}$ [D]	$m_{ee'}$ [D]
1				3.46	3.41	6.5 (6.2)	4.3 (6.4)	5.0 (9.1)
2	3.82	5.1	12.8					
3				3.49	3.59	11.2(10.8)	7.6 (4.9)	9.6 (6.9)
4	3.71	8.8	9.7					
5				2.46	3.56	8.9 (8.8)	7.1 (1.4)	8.7 (1.9)
6	2.95	7.2	2.7					
7				4.23	4.76	7.6 (7.8)	8.2 (4.1)	11.9 (5.7)
8	4.32	6.4	8.1					
9				2.21	2.96	10.5 [a]	4.5	10.1 [a]
						$m_{ge'}$=6.0 [b]		

[a] *y*-axis component (the *y* axis is defined as the axis passing through the two NEt_2 donor sites). [b] Because of the reduced dimensionality, the second excited state is also one-photon dipole allowed (along *x*).

  1616-301X/02/0909-0635 $ 17.50+.50/0

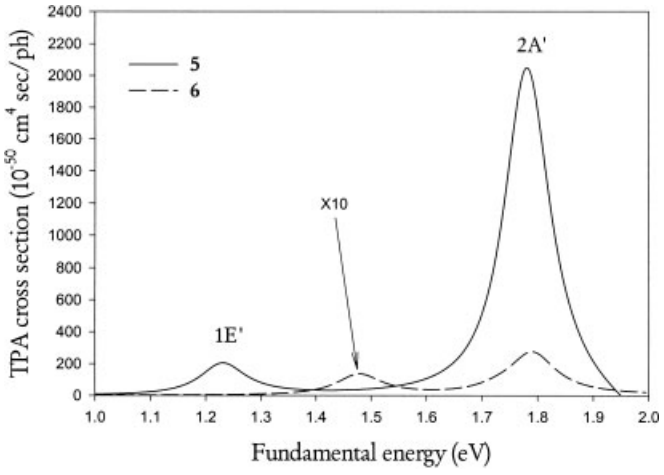

Fig. 4. INDO/MRD-CI/SOS two-photon absorption spectra of molecules **5** and **6**.

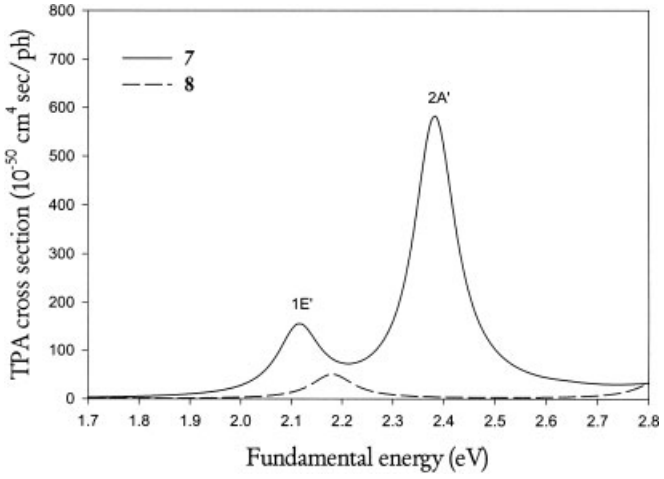

Fig. 5. INDO/MRD-CI/SOS two-photon absorption spectra of molecules **7** and **8**.

arms breaks down. The coupling between the three charge-transfer pathways of the molecule is strong, as demonstrated by the large inter-arm interaction energy: the splitting between the E′ and A′ states is calculated to be ~1.1 eV. Therefore, *two well-separated* two-photon absorption resonances are predicted in the low energy region of the TPA spectrum of **5**, instead of one in **1** and **3**. The matrix elements computed for the octupole are much larger than those predicted from the exciton approach and the TPA response of crystal violet is therefore strongly enhanced by comparison with its one-dimensional analog **6**. In fact, excitation from the ground state to the lowest excited state in **6** drives the positive charge, mainly localized on the phenylene ring in the ground state, to the CH_2 group; there is hardly any charge transfer involving the external amino group, which explains the small dipole moment difference in Table 1. The situation is different in **5**, where the excess charge is delocalized over the three aromatic rings (which adopt a slight quinoid character), and a significant amount of electron density is moved from the periphery towards the center of the molecule upon excitation. It is also worth noting that, although the dipole matrix elements are similar or even smaller than those obtained in **3**, crystal violet shows a larger TPA peak associated with resonance to 2A′. This mainly arises because of the detuning energy (difference between E(1E′) and E(2A′)/2), which amounts to ~0.7 eV in **5** and ~1.8 eV in **3** (see Eq. 7).

iv) The results obtained for molecule **7** are in line with those described above for crystal violet. The energy difference between the lowest two excited states (1E′ and 2A′) is large (~0.5 eV), indicating significant cross-talk between the three arms of the octupolar molecule. There is a large increase (by more than a factor 2) in the amount of donor-to-acceptor charge transfer per arm when switching from the dipolar compound **8** to the octupolar molecule **7**; this explains the higher dipole matrix elements computed at the INDO/MRD-CI level with respect to the values predicted on the basis of the charge distribution in **8** and the exciton model. As a result, the low-energy part of the TPA spectrum of **7** shows two separate peaks with peak δ values much higher than the values predicted from exciton theory.

From these results, it clearly appears that the amplitude of the TPA response in octupolar architectures can be modulated through the cross-talk between the three charge-transfer dipolar arms. The design of octupolar compounds with enhanced TPA cross sections requires the exploitation of cores that allow delocalization of the excited-state wavefunctions through strong inter-arm interactions (such a C^+ or N centers) and arms leading to an optimal ground-state polarization. The latter requirement can be achieved by using the design routes that have been successfully applied to the optimization of the second-order response of dipolar push–pull compounds.[24,25] Indeed, as for the one-dimensional non-centrosymmetric structures, the TPA response in octupoles is controlled by the amount of charge transfer from the ground state to the excited state, i.e., the difference in state dipole moment (although for strong coupling between the arms the description is probably more complex than that given by Eqs. A8 and A9 in the Appendix). As a consequence, the two-photon absorption cross section and the second-order molecular polarizability are expected to show the same dependence on chemical structure.[19]

We have applied the same INDO/MRD-CI methodology to describe the excited states and

Table 2. Excitation energies (and 1E<M>′–2A′ energy separation) and two-photon absorption cross sections in the octupolar compounds, as computed at the INDO/MRD-CI level. The experimental values for crystal violet and brilliant green in glycerol are indicated between parentheses. ω is the resonance energy.

Compound	1A′–1E′ [eV]	1A′–2A′ [eV]	1E′–2A′ [eV]	ω [eV]	δ [10^{-50} cm^4 s/ph)]
1	3.46	3.41	–0.05	1.72	74
3	3.49	3.59	0.1	1.79	583
5	2.46 (2.08)	3.56 (~3.3)	1.1 (1.2)	1.23	206
				1.78 (1.65)	2041 (1980)
7	4.23	4.76	0.53	2.11	154
				2.38	581
9	2.21 (1.95)	2.96 (2.85)	0.75 (0.9)	1.10	47
				1.48 (1.48)	852 (762)

  1616-301X/02/0909-0636 $ 17.50+.50/0 Adv. Funct. Mater. 2002, 12, No. 9, September

ADVANCED FUNCTIONAL MATERIALS

TPA spectrum of brilliant green, **9**. The reasons for looking into the nonlinear optical response of this molecule are twofold. First, due to the reduced symmetry of the compound, the selection rules for one- and two-photon excitations are expected to be somewhat relaxed, which should allow easy identification of all relevant excited states from linear absorption; in addition, due to the similar chemical structures of **9** and **5**, comparison between the one- and two-photon absorption spectra of crystal violet and brilliant green should provide rich insight into the nature of the lowest excited states in octupolar chromophores. Second, for a number of practical reasons, molecule **9** appears to be an interesting target molecule for TPA; the photophysics of compounds **5** and **9** have therefore been investigated experimentally.

The simulated TPA spectrum of **9** is shown in Figure 6. As for **5**, two peaks are calculated in the low energy part of the spectrum. From the comparison between the excitation energies, dipole matrix elements, and wavefunctions in molecules **5** and **9**, the excited states associated with the lowest two resonances in **9** can unambiguously be associated with the 1E′ and 2A′ states of the corresponding C_3-symmetry structure, i.e., **5**. The mechanism for the TPA response is reminiscent of that in crystal violet. Of course, because of the reduced symmetry, the pseudo 2A′ state in **9** is coupled optically to the electronic ground state through a significant oscillator strength. The excitation energies and dipole matrix elements between the relevant electronic states in **9**, as calculated at the INDO/MRD-CI level, are listed in Table 1.

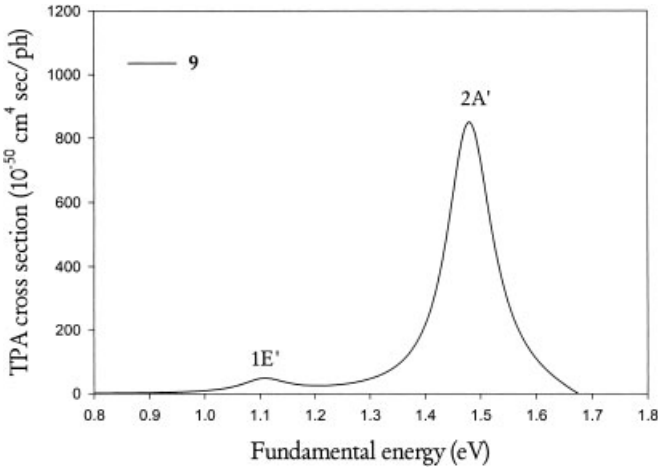

Fig. 6. INDO/MRD-CI/SOS two-photon absorption spectrum of molecule **9**.

With respect to **5**, the lowest two excited states are red shifted in **9** and their energy separation (related to the interarm coupling) is slightly reduced (from 1.1 eV in **5** to 0.8 eV in **9**). As a consequence of the reduced dimensionality, the *y*- and *x*-components (the *x*-axis is defined here as the axis from the central carbon site to the unsubstituted phenyl ring) of the third-order polarizability are not equivalent anymore (the isotropic response is actually dominated by the *yyyy* and *xxyy* tensor components). Because of weaker charge transfer from the periphery to the core of the molecule upon excitation, the state dipole moment difference (along *x*) is also smaller in **9** compared to **5**. Despite the fact that the transition dipole moments between the ground state and the lowest excited state and among the two lowest excited states are larger in **9** than in **5**, the decrease in dimensionality, the overall reduced charge transfer (as well as, to a lesser extent, the increased detuning energy) lead to TPA cross sections for both the first and second resonances in **9** that are smaller than in **5**, Table 2.

5. Experimental Study of TPA in Crystal Violet and Brilliant Green

The two-photon absorption cross sections of crystal violet, **5**, and brilliant green, **9** (Scheme 1) were measured by means of two-photon absorption induced fluorescence,[10] which yields a measure of the product $\eta\delta$ (with η the fluorescence quantum yield). Calibration against a compound with known $\eta\delta$, and a measurement of η (assumed to be the same after one- and two-photon excitations) then provides the δ value. While this is the most commonly used and well-proven principle for the measurement of TPA cross sections, two problems severely complicated such measurements for the molecules studied here. First, the fluorescence quantum yields (QY) of crystal violet and brilliant green are extremely low in liquid solution, limiting the sensitivity of the measurements. Second, because of the nearly doubly resonant nature of the two-photon transition, the two-photon absorption peak for these compounds occurs at a wavelength close to the linear absorption band. Therefore, great care needs to be taken to distinguish the two-photon excited fluorescence from possible spurious signals due to residual absorption in the long wavelength tail of the linear absorption band.

The low fluorescence QY of triarylmethane dyes, attributed to a radiationless relaxation process involving a rotation of the phenyl groups, is known to increase significantly with solvent viscosity.[33] Therefore, the TPA measurements were performed in a highly viscous solvent, glycerol. As the viscosity is temperature dependent, the fluorescence QY of both compounds in glycerol was measured as a function of temperature and the temperature at which the TPA experiments were performed was recorded.

The linear absorption spectrum of **5**, as measured in glycerol, is shown in Figure 7. The low-energy part of the spectrum shows a dominant peak at 2.08 eV (597 nm), which can be readily attributed to optical transition from the ground state to the lowest doubly degenerate E′ excited state. Note that the calculated 1A′–1E′ transition energy, 2.46 eV, is in good agreement with the spectroscopic value. A much weaker feature is measured at ~3.3–3.5 eV (376–359 nm) that we assign to the one-photon electronic excitation to the 2A′ excited state (calculated at 3.56 eV). As pointed out above, such a transition is dipole forbidden in a $C(D)_{3(h)}$ molecule but might become partially allowed upon relaxation of the molecular geometry to a conformation with lower symmetry. This assignment is supported by:

- the very weak optical cross section measured for this transition, which is consistent with a symmetry-forbidden excita-

  1616-301X/02/0909-0637 $ 17.50+.50/0

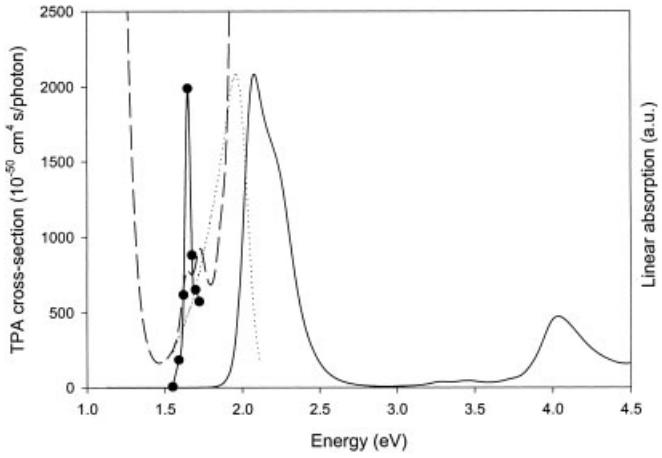

Fig. 7. Linear absorption (solid line), emission (dotted line), and two-photon absorption (circles; the connecting line is a guide to the eye) spectra of crystal violet, **5**, in glycerol. The dashed line is an enlargement (30×) of the weak linear absorption bands in the range ~350–400 nm, plotted versus twice the wavelength, for easy comparison with the TPA spectrum.

tion (the extinction coefficient is almost two orders of magnitude smaller at 3.30 eV than at 2.08 eV);

- the excellent agreement with the INDO/MRD-CI calculated energetic position for the 2A′ excited state and the resulting 1E′–2A′ energy separation (in excess of 1 eV).

In addition, the changes in optical spectrum when going from **5** to **9** are fully consistent with the theoretical predictions, Figure 8:

- two bands (a strong one that peaks at 1.95 eV and a weak one at 2.85 eV) are measured in the visible range for **9**, which are both red shifted in comparison to **5**;
- the energy difference between the first two excited states, which correspond to the 1E′ and 2A′ states of crystal violet, is reduced from ~1.2 eV in **5** to ~0.9 eV in **9**, in remarkable agreement with the shifts predicted at the INDO/MRD-CI level (1.1 eV in **5** and 0.8 eV in **5**).

The experimental two-photon absorption spectra of compounds **5** and **9** are shown in Figures 7 and 8. Peak TPA cross sections of 762×10^{-50} cm^4 s/photon and 673×10^{-50} cm^4 s/photon ($\eta\delta = 23.4 \times 10^{-50}$ cm^4 s/photon and 20.7×10^{-50} cm^4 s/photon) were found in brilliant green for laser wavelengths of 840 nm and 880 nm, respectively. This wavelength range matches well with the position of the second linear absorption band. The twin structure of the TPA spectrum is likely related to coupling to vibrational modes, although there are other possible scenarios (such as the presence of two distinct conformers). The TPA spectrum of crystal violet shows a strong peak with $\delta = 1980 \times 10^{-50}$ cm^4 s/photon ($\eta\delta = 36.6 \times 1\,10^{-50}$ cm^4 s/photon) for an incident wavelength of 752 nm, in agreement with the position of the weak linear absorption band at 376 nm, which we assign to the 1A′–2A′ transition. We also observed a weak TPA at around 1200 nm (1.04 eV), corresponding to the two-photon resonance into 1E′, but we were unable to quantify the TPA cross section in this wavelength range because the data for the reference standards were only available up to 1050 nm. The fact that the 1E′ state is two-photon allowed also explains the problems due to spurious fluorescence contributions observed in hyper-Rayleigh scattering measurements using a fundamental wavelength of 1064 nm.[34]

The δ values measured when resonance into the second (2A′) excited state is achieved are in excellent agreement with the theoretical values and, in particular, show the same trend (increase) from **9** to **5**, Table 2 (although a direct comparison should be made with caution since the calculated values are sensitive to the actual choice of the damping factors and local field factors as well as vibronic coupling have not been included in the theoretical model). Most importantly, the experimental data reported here:

- provide further evidence for the theoretical model of TPA in octupolar compounds; in particular, it is found that interactions among the arms of crystal violet and (to a lesser extent) brilliant green remove the degeneracy between the lowest excited states and boost the TPA cross section associated with the higher lying 2A′ state;
- confirm the high potential of octupolar structures as TPA-active materials.

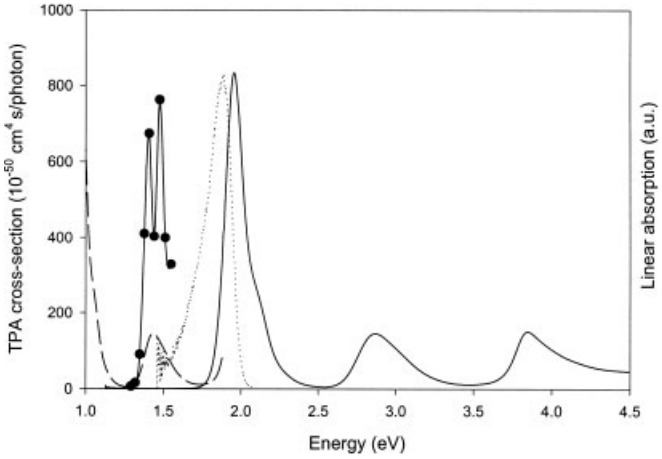

Fig. 8. Linear absorption (solid line), emission (dotted line), and two-photon absorption (circles; the connecting line is a guide to the eye) spectra of brilliant green, **9**, in glycerol. The dashed line is a plot of the weaker linear absorption band versus twice the wavelength, for easy comparison with the TPA spectrum.

6. Conclusions

On the basis of a correlated description of the excited states, a perturbative analysis of the two-photon absorption properties of octupolar structures has been performed. We have first developed a simple exciton model allowing insight into the mechanism for two-photon absorption in C_3-symmetry architectures to be gained, where charge transfer takes place along three main charge-transfer axes. According to the exciton picture (which is applicable in the case of weak coupling among the three arms of the C_3 structure), the TPA cross section, δ, in the octupoles should scale as three times the corresponding values in the isolated dipolar arms. As for their one-dimensional analogs, the amount of charge transferred when going from the ground state to the excited state (and the resulting difference in state dipole moment) is the most relevant ingredient for the achievement of high δ values.

  1616-301X/02/0909-0638 $ 17.50+.50/0 Adv. Funct. Mater. 2002, 12, No. 9, September

ADVANCED FUNCTIONAL MATERIALS

Quantum-chemical calculations performed on the full chemical structure of a few representative octupolar molecules confirm the predictions of exciton theory in the limit of weak inter-arm couplings; this is for instance the case of a benzene-core chromophore bearing substituents in meta positions. Note that deviations from the factor 3 increase in δ can be accounted for in the exciton model by injecting the actual amount of charge transfer (i.e., the degree of ground-state polarization) as calculated in the octupolar compound (the factor 3 enhancement is recovered when the magnitude of the donor-to-acceptor charge transfer summed over the three arms of the octupole is identical to that taking place in the isolated conjugated branches).

The "supermolecular" calculations also suggest that much larger enhancement factors can be achieved through proper design of the core of the chromophore, allowing efficient cross-talk among the conjugated arms. This is for instance the case of crystal violet, for which δ is increased by more than one order of magnitude with respect to its one-dimensional counterpart. Strong inter-arm interactions lead to a splitting of the 1E′/2A′ excited-state energies and the appearance of *two* two-photon resonances on the low energy part of the TPA spectrum. For both resonances, the magnitude of the TPA response is controlled primarily by the dipole matrix elements from the ground state and among the lowest excited states, which to a large extent can be related to the state dipole difference in the isolated arms. As a consequence, the second-order molecular polarizability and the two-photon absorption cross section to the 1E′ and 2A′ states are predicted to evolve in parallel in octupolar molecules. In addition, in the case of large inter-arm couplings (such as that calculated for molecule **5**), the peak δ value is expected to be higher at the 2A′ resonance, as a result of a smaller detuning energy. Whether one can take advantage of this effect depends on the actual width of the absorption lines, since broad lines would result in significant linear absorption at the input pump frequency.

The potential of octupolar molecules as TPA-active materials is supported by measurements on crystal violet, showing δ values in the 2A′ state comparable to those reported for quadrupolar[11,12,35,36] and dipolar[13,37,38] architectures. This is quite remarkable since no effort to optimize the TPA response in this class of materials has been made and crystal violet is therefore unlikely to be an optimal molecule. In addition, the description of the excited states as accessed by one- and two-photon absorption spectroscopies confirms the mechanisms for two-photon absorption in C_3-symmetry molecules, as laid down by the quantum-chemical calculations. In particular, they are consistent with the emergence of two excited states in the octupole that are both two-photon allowed; these excited states stem from the interactions between the three charge-transfer channels.

It would be most interesting to extend this study to the higher lying excited states of the one-dimensional systems (in particular the second excited state, reminiscent of the $2A_g$ state of stilbene and centrosymmetric derivatives, for which high TPA cross sections have been reported)[11] and their counterparts in the octupolar chromophores. From the present work, the combination of dimensionality and the pronounced electron density migration associated with excitation in the higher lying excited states of phenylene-based oligomers is expected to yield record δ values in octupolar molecules wherein a central core such as a positively charged carbon atom or a nitrogen (to promote inter-arm interactions) bears three phenylenevinylene-based conjugated segments end-capped with strong donor groups (to tune the ground-state polarization). We are currently investigating this type of architectures.

7. Experimental

Compounds were obtained from Aldrich (crystal violet, brilliant green) or Acros (coumarin 307, rhodamine B) and dissolved in spectrophotometric grade solvents (Aldrich). For TPA measurements, concentrations in the range from 8×10^{-7} to 1×10^{-5} M were used.

The two-photon absorption measurements on brilliant green were performed with femtosecond mode-locked laser pulses using a Ti:sapphire laser (Spectra-Physics Tsunami, using broadband optics) pumped by a diode pumped Nd:YVO_4 laser (Spectra-Physics, Millennia V). The laser beam (up to ~100 mW average power, ~100 fs, 82 MHz repetition rate, λ = 800–940 nm, vertical polarization) was focused into a 1 cm path length glass sample cell, using an ~*f*/15 focusing geometry so that the entire focal region fitted well within the 1 cm path length. Two-photon excited fluorescence was collected at 90° to the incident beam, imaged onto the horizontal entrance slit of a monochromator, and detected with a photomultiplier operated in single photon counting mode. The incident laser beam was aligned close (0.3 to 1 mm) to the emission collection window of the cell so that reabsorption of fluorescence was negligible at the concentrations used. Short wavelength passing interference filters were placed in front of the monochromator entrance to fully eliminate scattered laser light.

Rhodamine B in methanol was chosen as the reference standard [10] because its emission band overlaps with that of brilliant green, allowing us to use the same detection wavelength (650 nm and 690 nm) for both compounds. This monochromatic detection eliminates the need to correct for the wavelength dependence of the monochromator and photomultiplier efficiency. Two-photon absorption cross sections are then derived as:

$$\delta_s^{(\lambda)} = \frac{N_{ref}}{N_s}\frac{C_{ref}}{C_s}\frac{\eta_{ref}}{\eta_s}\frac{\int F_s}{F_s(\lambda')}\frac{F_{ref}(\lambda')}{\int F_{ref}}\frac{S_s}{S_{ref}}\delta_{ref}^{(\lambda)} \quad (8)$$

where subscripts s and ref refer to the "unknown" (brilliant green) sample and reference sample, respectively; C_i are the molar concentrations, S_i the measured signals, λ is the laser wavelength, and λ' the emission detection wavelength; $F_i(\lambda)$ are the fluorescence emission spectra (as measured with a Fluorolog II fluorometer), used to relate the detected two-photon excited emission intensity at a single wavelength to the total emission. The N terms are correction factors that account for the different refractive indices of the solvents used, which influence both the focusing of the incident beam and the effective collection angle of the fluorescence light (as well as causing minute changes in the reflection, hence to the transmission T, at the windows for both laser and fluorescence lights). These factors are given by:

$$N = \frac{n_\lambda}{n_{\lambda'}^2}T_\lambda^2 T_{\lambda'} \quad (9)$$

where all refractive indices are taken to be n_D of the solvent (neglecting dispersion).

The set-up used for two-photon absorption measurements on crystal violet is shown in Figure 9. Pulses from a mode-locked Ti:sapphire laser (Spectra Physics Tsunami, pumped by Spectra Physics Millennia V) are amplified and recompressed by a stretched pulse regenerative Ti:sapphire amplifier (Spectra-Physics Spitfire), which is pumped by a diode-pumped Nd:YLF laser (Spectra-Physics Evolution). The amplified pulses (800 nm, 1 kHz, ~120 fs) are used to pump an optical parametric amplifier (Spectra-Physics OPA-800CFP), the signal output beam of which is frequency doubled to give femtosecond pulses tunable over the wavelength range of 600–800 nm. This beam was slightly apertured down to improve beam quality, and spectrally filtered as shown in Figure 9 using two 60° prisms (BK7) spaced ~85 cm, and a 0.5 mm slit in front of a retroreflecting mirror. This geometry also acts as a negative group velocity dispersion element, partially compensating for pulse broadening in the various other optical components

  1616-301X/02/0909-0639 $ 17.50+.50/0

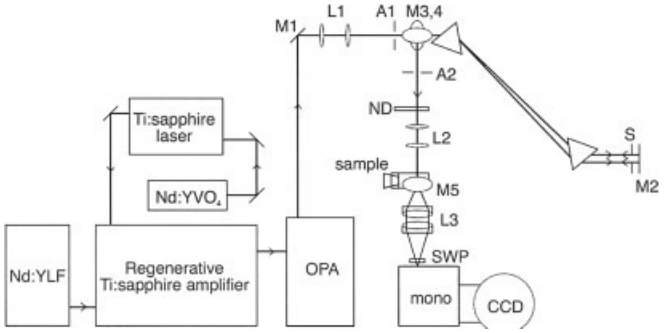

Fig. 9. Experimental set-up used for the TPA measurements on crystal violet. M*i*: mirrors; A*i*: diaphragms (~2–3 mm diameter); S: 0.5 mm slit on translation stage; M3,4: periscope (changing the polarization from vertical to horizontal); ND: variable reflective attenuator; L1: lens system collimating/slightly focusing beam onto slit S; L2: lenses focussing laser beam on sample; mirror M5 (ellipse above sample) directs laser beam vertically down through sample cell; L3: lenses collecting and imaging fluorescence light onto monochromator (mono); SWP: short wavelength passing filters.

of the set-up. The spectra of the excitation light after this filtering were typically ~15 nm (FWHM) wide, and approximately Gaussian in shape. A weak (order of *f*/50) focusing resulted in an essentially collimated beam over the 1 cm path length of the sample cell.

Two-photon excited fluorescence was again collected at 90°, and the emission spectrum recorded using a monochromator (Acton SpectraPro-150, with 300 lines/mm grating) with liquid nitrogen cooled charge coupled device (CCD) detector (Princeton Instruments LN/CCD-1100-PB). The emission spectra were corrected for the wavelength dependence of the monochromator and detector efficiency based on a measurement of the emission (one-photon excited by the fourth harmonic of the OPA signal beam) of a dye with known, broad emission spectrum (dansyl hydrazine in methanol, using a corrected fluorescence spectrum obtained with a Spex Fluorolog II fluorometer). The corrected two-photon excited emission spectra were integrated over part of the emission band (up to ~670 nm, as in the long wavelength tail of the emission scattered laser light interferes with the measurement), and the missing fraction of the integrals was factored in, based on the known (one-photon excited) emission spectra of the compounds. These corrected integrals are then used as a measure of $NC\eta\delta$, where N is now adapted to account for a collimated rather than a focused laser beam:

$$N = \frac{1}{n_{\lambda'}^2} T_{\lambda}^2 T_{\lambda'} \tag{10}$$

Measurements were calibrated against coumarin 307 in methanol [10]. The low average laser powers used (< 1 mW), the low absorbance, and the observed quadratic power dependence ensured that heating by the laser beam was negligible.

Fluorescence quantum yields were referenced at one temperature to Nile blue A perchlorate in ethanol (QY = 0.27 at 24 °C), and the temperature dependence of the QY was obtained by monitoring the relative emission intensity at the peak emission wavelength. Small changes in the shape of the emission spectrum were observed, but the effect (< 3 % over the range 21–30 °C) of these changes on the QY was neglected. Quantum yields thus obtained for brilliant green and crystal violet in glycerol, at the temperatures at which the TPA measurements were performed [(20 ± 1) °C and (22.2 ± 0.3) °C, respectively] were 0.0307 and 0.0185, respectively (for crystal violet in glycerol at 25 °C, we obtain a QY of 0.0149, which compares to a value of 0.019 reported by Brey et al. [30]. Given the many experimental difficulties (low and temperature-dependent fluorescence quantum yield, proximity of linear absorption band), the experimental uncertainty on the TPA cross sections is estimated to be on the order of 40 %.

8. Appendix: Molecular Exciton Model for Octupolar Systems

We start with the assumption that the wavefunctions of the ground state and excited states of the octupolar molecules can be built as an ad hoc linear combination of the isolated-arm wavefunctions, which implies weak interactions between the arms of the octupolar system [31]. That is to say (for C_{3h} chromophores) that the following expressions:

$$\begin{aligned}
&|1A'\rangle = |a^0\rangle|b^0\rangle|c^0\rangle \\
&|2A'\rangle = \frac{1}{\sqrt{3}}\left(|a^*\rangle|b^0\rangle|c^0\rangle + |a^0\rangle|b^*\rangle|c^0\rangle + |a^0\rangle|b^0\rangle|c^*\rangle\right) \\
&|1E'_{\alpha}\rangle = \frac{1}{\sqrt{6}}\left(2\times|a^*\rangle|b^0\rangle|c^0\rangle - |a^0\rangle|b^*\rangle|c^0\rangle - |a^0\rangle|b^0\rangle|c^*\rangle\right) \\
&|1E'_{\beta}\rangle = \frac{1}{\sqrt{2}}\left(|a^0\rangle|b^*\rangle|c^0\rangle - |a^0\rangle|b^0\rangle|c^*\rangle\right)
\end{aligned} \tag{A1}$$

describe the 1A′ ground-state, the 2A′ excited-state, and the doubly degenerate 1E′ excited-state wavefunctions of the octupolar compound, respectively (with $|a^0\rangle$ the ground state and $|a^*\rangle$ the excited state of arm a, etc).

These expressions can then be used to relate the state and transition dipole moments of the octupolar compounds in terms of the molecular parameters associated with the individual arms (M_{ge} and $\delta\mu_{ge}$). For the dipole matrix elements, one readily obtains:

- the transition moments from the ground state:

$$\begin{aligned}
&\langle GS|\mu_x|2A'\rangle = \langle GS|\mu_y|2A'\rangle = \langle GS|\mu_z|2A'\rangle = 0 \\
&\langle GS|\mu_x|1E'_{\alpha}\rangle = \sqrt{\frac{3}{2}}M_{ge}, \ \langle GS|\mu_y|1E'_{\alpha}\rangle = \langle GS|\mu_z|1E'_{\alpha}\rangle = 0 \\
&\langle GS|\mu_y|1E'_{\beta}\rangle = -\sqrt{\frac{3}{2}}M_{ge}, \ \langle GS|\mu_x|1E'_{\beta}\rangle = \langle GS|\mu_z|1E'_{\beta}\rangle = 0
\end{aligned} \tag{A2}$$

we note that the oscillator strength in the octupole (sum over the squared transition dipole components) is then exactly three times that of the individual arms; in addition, the electronic transition from the ground state to the 2A′ state is one-photon forbidden;

- the transition moments among excited states:

$$\begin{aligned}
&\langle 1E'_{\alpha}|\mu_x|2A'\rangle = \sqrt{\frac{1}{2}}\Delta\mu_{ge}, \langle 1E'_{\alpha}|\mu_y|2A'\rangle = \langle 1E'_{\alpha}|\mu_z|2A'\rangle = 0 \\
&\langle 1E'_{\beta}|\mu_y|2A'\rangle = -\sqrt{\frac{1}{2}}\Delta\mu_{ge}, \langle 1E'_{\beta}|\mu_x|2A'\rangle = \langle 1E'_{\beta}|\mu_z|2A'\rangle = 0 \\
&\langle 1E'_{\alpha}|\mu_y|1E'_{\beta}\rangle = \frac{1}{2}\Delta\mu_{ge}, \langle 1E'_{\alpha}|\mu_x|1E'_{\beta}\rangle = \langle 1E'_{\alpha}|\mu_z|1E'_{\beta}\rangle = 0
\end{aligned} \tag{A3}$$

- the state dipoles:

$$\begin{aligned}
&\langle 1A'|\mu_x|1A'\rangle = \langle 1A'|\mu_y|1A'\rangle = \langle 1A'|\mu_z|1A'\rangle = 0 \\
&\langle 1E'_{\alpha}|\mu_x|1E'_{\alpha}\rangle = \frac{1}{2}\Delta\mu_{ge}, \langle 1E'_{\alpha}|\mu_y|1E'_{\alpha}\rangle = \langle 1E'_{\alpha}|\mu_z|1E'_{\alpha}\rangle = 0 \\
&\langle 1E'_{\beta}|\mu_x|1E'_{\beta}\rangle = -\frac{1}{2}\Delta\mu_{ge}, \langle 1E'_{\beta}|\mu_y|1E'_{\beta}\rangle = \langle 1E'_{\beta}|\mu_z|1E'_{\beta}\rangle = 0
\end{aligned} \tag{A4}$$

The excitation energies can be estimated on the basis of the expressions for the wavefunctions given above (Eq. A1). We first assume that there is no interaction among the arms, that is to say the total Hamiltonian H is given by: $H = H_a + H_b + H_c$ (with all interaction terms H_{ij}, with i,j = a–c, set to zero). Denoting the ground-state energy of each arm as E^0 and its excited-state energy E^* (the excitation energy within each arm is thus given by $E^*–E^0$), the ground-state and excited-state energies of the octupole can be written:

$$\begin{aligned}
&\langle 1A'|H|1A'\rangle = 3\times E^0 \\
&\langle 1E'_{\alpha}|H|1E'_{\alpha}\rangle = \langle 1E'_{\beta}|H|1E'_{\beta}\rangle = 2\times E^0 + E^*; \langle 2A'|H|2A'\rangle = 2\times E^0 + E^*
\end{aligned} \tag{A5}$$

In this case, the excitation energies are exactly the same as those obtained for the dipolar arms, i.e., $E^*–E^0$, and the transitions to the 2A′ and 1E′ states are (accidentally) degenerate. If we now include the interaction terms ($H_{ij} = V$ for any i,j), the excited-state energies can be expressed as (neglecting polarization effects):

$$\begin{aligned}
&\langle 1E'_{\alpha}|H|1E'_{\alpha}\rangle = \langle 1E'_{\beta}|H|1E'_{\beta}\rangle = 2\times E^0 + E^* - V \\
&\langle 2A'|H|2A'\rangle = 2\times E^0 + E^* + 2\times V
\end{aligned} \tag{A6}$$

with $V = \langle a^*|\langle b^0|H|b^*\rangle|a^0\rangle$ the coupling energy between excited states localized on separate arms (in the point-dipole approximation, V is proportional to the square of the single-arm transition moment, M_{ge}) [31]. Therefore, interac-

  1616-301X/02/0909-0640 $ 17.50+.50/0 *Adv. Funct. Mater.* **2002**, *12*, No. 9, September

tion between the three charge-transfer paths is expected to remove the degeneracy between the 1E′ and 2A′ states, which become split by three times the inter-arm coupling energy V in the octupole.

By symmetry, the average value of the third-order molecular polarizability (and therefore also of the TPA cross section) in three-fold symmetry compounds is 8/15 times the (x-)longitudinal component. In the limit of very weak interaction among the arms, the splitting between E′ and A′ states in the octupolar chromophore is expected to be vanishingly small (Eq. A5 holds) and the transition energies to the 1E′ and 2A′ excited states should be close to the corresponding value in the isolated arm. Therefore, both the dipolar D and two-photon T terms in Equation 2 will be resonantly enhanced through a two-photon absorption phenomenon with an incoming light of half the excitation energy to the nearly degenerate 2A′ and 1E′ excited states. In this limiting case, the longitudinal TPA cross section at the peak position of the two-photon resonance is proportional to (sum of Eqs. 3 and 4 when $E_{ge} \rightarrow E_{ge'}$):

$$\frac{m_{ge}^2(\delta\,\mu_{ge}^2 + m_{ee'}^2)}{(\frac{\varepsilon_{ge}}{2})^2\Gamma} \tag{A7}$$

where small letters refer to molecular parameters in the octupole; $|e>$ denotes the doubly degenerate E′ excited state and $|e'>$ corresponds to the 2A′ excited state. On the basis of the relationships between the dipole matrix elements in the octupole and in the individual charge-transfer arms (Eqs. A2 to A4), Equation A7 can be rewritten as:

$$\frac{M_{ge}^2(\frac{3}{8}\Delta\mu_{ge}^2 + \frac{3}{4}\Delta\mu_{ge}^2)}{(\frac{E_{ge}}{2})^2\,\Gamma} = \frac{9}{8}\frac{M_{ge}^2\Delta\mu_{ge}^2}{(\frac{E_{ge}}{2})^2\,\Gamma} \tag{A8}$$

where capital letters refer to excitation energies, state, and transition dipole moments in the dipolar arm. In more general cases (when V is non-negligible with respect to the line width, so that resonances to the 1E′ and 2A′ excited states can be distinguished), the expressions for the TPA cross sections into the 1E′ and 2A′ excited states can be written as:

$$\delta_{1E'} \propto \frac{3}{8}\frac{M_{ge}^2\Delta\mu_{ge}^2}{(\frac{E_{ge}-V}{2})^2\,\Gamma} \qquad \delta_{2A'} \propto \frac{6}{8}\frac{M_{ge}^2\Delta\mu_{ge}^2}{(\frac{E_{ge}}{2}-2V)^2\Gamma} \tag{A9}$$

It is interesting to note that we can obtain some insight into the effect of modulating the total amount of charge transfer along the three axes of the octupolar compound by artificially changing the value of $\Delta\mu_{ge}$ in Equation A8. Since $\delta \propto \delta\mu_{ge}{}^2$ and $\Delta\mu_{ge} \propto q$ (with q the amount of charge transferred from donor to acceptor along each octupolar axis), it follows that the TPA cross section depends on q^2 (assuming that all other molecular parameters do not depend on q). When the amount of charge transfer per arm summed over the 1E′ and 2A′ excited states in the octupolar molecule is similar to the ground-to-lowest excited state charge transfer in the corresponding one-dimensional dipolar arm ($q = q_0$), we recover the factor 3 increase in δ when switching from dipolar to octupolar architecture; a reduction by 30 % of the charge transfer reduces δ by about a factor 2 while doubling q would result in a four-fold increase in δ.

Received: February 5, 2002
Final version: May 27, 2002

[1] W. Denk, J. H. Strickler, W. W. Webb, *Science* **1990**, *248*, 73.
[2] P. M. Rentzepis, S. D. A. Parthenopoulos, *Science* **1989**, *245*, 843.
[3] J. E. Ehrlich, X. L. Wu, I.-Y. S. Lee, Z.-H. Hu, H. Röckel, S. R. Marder, J. W. Perry, *Opt. Lett.* **1997**, *22*, 1843.
[4] A. A. Said, C. Wamsely, D. J. Hagan, E. W. Van Stryland, B. A. Reinhardt, P. Roderer, A. G. Dillard, *Chem. Phys. Lett.* **1994**, *228*, 646.
[5] G. S. He, R. Gvishi, P. N. Prasad, B. Reinhardt, *Opt. Commun.* **1995**, *117*, 133.
[6] D. A. Parthenopoulos, P. M. Rentzepis, *Science* **1989**, *245*, 843.
[7] J. H. Strickler, W. W. Webb, *Opt. Lett.* **1991**, *16*, 1780.
[8] D. L. Pettit, S. S. H. Wang, K. R. Gee, G. J. Augustine, *Neuron* **1997**, *19*, 465.
[9] B. H. Cumpston, S. P. Anthavel, S. Barlow, D. L. Dyer, J. E. Ehrlich, L. L. Erskine, A. A. Heikal, S. M. Kuebler, I.-Y. S. Lee, D. McCord-Maughon, J. Qin, H. Röckel, M. Rumi, X.-L. Wu, S. R. Marder, J. W. Perry, *Nature* **1999**, *398*, 51.
[10] C. Wu, W. W. Webb, *J. Opt. Soc. Am. B* **1996**, *13*, 481.
[11] M. Albota, D. Beljonne, J.-L. Brédas, J. E. Ehrlich, J.-Y. Fu, A. A. Heikal, S. E. Hess, T. Kogej, M. D. Levin, S. R. Marder, D. McCord-Maughon, J. W. Perry, H. Röckel, M. Rumi, G. Subramaniam, W. W. Webb, X.-L. Wu, C. Xu, *Science* **1998**, *281*, 1653.
[12] M. Rumi, J. E. Ehrlich, A. A. Heikal, J. W. Perry, S. Barlow, Z. Y. Hu, D. McCord-Maughon, H. Röckel, S. Thayumanavan, S. R. Marder, D. Beljonne, J.-L. Brédas, *J. Am. Chem. Soc.* **2000**, *122*, 9500.
[13] T. Kogej, D. Beljonne, F. Meyers, J. W. Perry, S. R. Marder, J.-L. Brédas, *Chem. Phys. Lett.* **1998**, *298*, 1.
[14] J. Zyss, *J. Chem. Phys.* **1993**, *98*, 6583.
[15] J. Zyss, I. Ledoux, *Chem. Rev.* **1994**, *94*, 77.
[16] J.-L. Brédas, F. Meyers, B. M. Pierce, J. Zyss, *J. Am. Chem. Soc.* **1992**, *114*, 4928.
[17] Y.-K. Lee, S.-L. Jeon, M. Cho, *J. Am. Chem. Soc.* **1998**, *120*, 10 921.
[18] W. Zhu, G. Wu, *J. Phys. Chem. A* **2001**, *105*, 9568.
[19] a) B. R. Cho, K. H. Son, S. H. Lee, Y.-S. Song, Y.-K. Lee, S.-J. Jeon, J. H. Choi, H. Lee, M. Cho, *J. Am. Chem. Soc.* **2001**, *123*, 10 039. b) W.-H. Lee, H. Lee, J.-A. Kim, J.-H. Choi, M. Cho, S.-J. Jeon, B. R. Cho, *J. Am. Chem. Soc.* **2001**, *123*, 10 658.
[20] M. Cha, W. E. Torruellas, G. I. Stegeman, W. H. G. Horsthuis, G. R. Möhlmann, J. Meth, *Appl. Phys. Lett.* **1994**, *65*, 2648.
[21] E. Zojer, D. Beljonne, T. Kogej, H. Vogel, S. R. Marder, J. W. Perry, J.-L. Brédas, *J. Chem. Phys.*, in press.
[22] S. R. Marder, J. W. Perry, J. L. Brédas, D. McCard-Maughen, M. E. Dickinson, S. E. Fraser, D. Beljonne, T. Kogej, in *Conjugated Oligomers, Polymers, and Dendrimers: From Polyacetylene to DNA* (Ed: J.-L. Brédas), De Boeck, Louvain-la-Neuve **1999**, p. 395.
[23] B. J. Orr, J. F. Ward, *Mol. Phys.* **1971**, *20*, 513.
[24] F. Meyers, S. R. Marder, B. M. Pierce, J.-L. Brédas, *J. Am. Chem. Soc.* **1994**, *116*, 10 703.
[25] J. L. Oudar, D. S. Chemla, *J. Chem. Phys.* **1977**, *66*, 2664.
[26] a) M. C. Zerner, G. H. Loew, R. F. Kichner, U. T. Mueller-Westerhoff, *J. Am. Chem. Soc.* **1980**, *102*, 589. b) J. E. Ridley, M. C. Zerner, *Theor. Chim. Acta* **1973**, *32*, 111.
[27] N. Mataga, K. Nishimoto, *Z. Phys. Chem.* **1957**, *13*, 140.
[28] a) K. Ohno, *Theor. Chem. Acta* **1964**, *2*, 219. b) G. Klopman, *J. Am. Chem. Soc.* **1964**, *86*, 4550.
[29] M. J. S. Dewar, E. G. Zoebisch, E. F. Healy, J. J. P. Stewart, *J. Am. Chem. Soc.* **1995**, *107*, 3902.
[30] a) *Electronic Processes in Organic Materials* (Eds: M. Pope, C. Swenberg), Oxford University Press, New York **1982**. b) *Electronic Processes in Organic Crystals and Polymers* (Eds: M. Pope, C. Swenberg), Oxford University Press, New York **1999**.
[31] M. Joffre, D. Yaron, R. J. Silbey, J. Zyss, *J. Chem. Phys.* **1992**, *97*, 56.
[32] D. Beljonne, unpublished.
[33] L. A. Brey, G. B. Schuster, H. G. Drickamer, *J. Chem. Phys.* **1977**, *67*, 2648.
[34] T. W. Chui, K. Y. Wong, *J. Chem. Phys.* **1998**, *109*, 1391.
[35] X. M. Wang, D. Wang, G. Y. Zhou, W. T. Yu, Y. F. Zhou, Q. Fang, M. H. Jiang, *J. Mater. Chem.* **2001**, *11*, 1600.
[36] L. Ventelon, L. Moreaux, J. Mertz, M. Blanchard-Desce, *Chem. Commun.* **1999**, 2055.
[37] B. A. Reinhardt, L. L. Brott, S. J. Clarson, A. G. Dillard, J. C. Bhatt, R. Kannan, L. Yuan, G. S. He, P. N. Prasad, *Chem. Mater.* **1998**, *10*, 1863.
[38] K. D. Belfield, D. J. Hagan, E. W. Van Stryland, K. J. Schafer, R. A. Negres, *Org. Lett.* **1999**, *1*, 1575.

  1616-301X/02/0909-0641 $ 17.50+.50/0